

Helium trimers and tetramers in two dimensions and quasi-two-dimensions

L. Vranješ^{1,2,*} and S. Kilić^{1,†}

¹*Faculty of Natural Sciences, University of Split, 21000 Split, Croatia*

²*Institut für Theoretische Physik, Johannes Kepler Universität, A 4040 Linz, Austria*

(Received 21 September 2001; published 1 April 2002)

The ground-state properties of ^3He and ^4He trimers and tetramers in infinite and restricted two-dimensional and quasi-two-dimensional (2D) space are studied. Using Monte Carlo calculation in two stages successively, simple variational Monte Carlo and diffusion Monte Carlo, we find that all trimers (except one of ^3He with spin 3/2) and tetramers are bound. In infinite 2D space the binding energy of ^4He trimer is $-183(1)$ mK and of tetramer $-435(1)$ mK. In the same environment for ^3He , using Jastrow-Feenberg-Bruch wave functions trimer (spin 1/2) is bound with $-0.013(1)$ mK and tetramer with $-0.021(1)$ mK. Employing in the same procedure “dimerlike” wave functions for ^3He molecules in infinite 2D space it is discovered that trimer prefers the structure of one dimer and one separate particle while a composition of two separate dimers is preferable for tetramer. In this case binding energies are $-0.020(1)$ mK for trimer and $-0.040(1)$ mK for tetramer. The binding energies of mixed molecules in infinite 2D space are $-74.3(4)$ mK ($^3\text{He}-^4\text{He}_2$); $-14(1)$ mK ($^3\text{He}_2-^4\text{He}$); $-254(4)$ mK ($^3\text{He}-^4\text{He}_3$); $-118(2)$ mK ($^3\text{He}_2-^4\text{He}_2$); $-11(1)$ mK ($^3\text{He}_3-^4\text{He}$). In holding potentials with well-adjusted parameters there is a drastic increase of binding for trimer and tetramer in both sorts of helium atoms.

DOI: 10.1103/PhysRevA.65.042506

PACS number(s): 31.15.Pf, 36.90.+f, 31.15.Ar

I. INTRODUCTION

Helium trimers and tetramers in infinite space have been the subject of research since the 1960s [1–11]. Experimental detection of helium-4 dimers and trimers [12–14] initiated further consideration of these and related systems.

In three dimensions (3D) many ground-state calculations of $^4\text{He}_N$ system, have shown the existence of binding for any N [15–20]. In particular, there are extensive calculations for ^4He trimer [21–28] showing the existence of two bound states of angular momentum 0. The excited state is especially interesting because of the possible manifestation of Efimov effect [29]. The recent studies disagree on whether the bound state with nonzero total angular momentum exists [22,25,30,31].

Due to the small ^3He mass and the Pauli principle among all other possible helium trimers only $^3\text{He}-^4\text{He}_2$ is bound in 3D [21,22,31,32].

Cramer, Bruch, and Cabral [5] constructed a form of fermion-trimer wave function and showed that binding of ^3He trimer was not possible in 3D. The same was shown for fermion tetramer by Nakaishi-Maeda and co-workers. [11]. In a series of papers [15,33–36] a minimum number of ^3He atoms that form a bound cluster in 3D was found to be between 20 and 40. The recent calculations [37,38] showed that this minimum number is 35.

The difference in binding properties in 3D and 2D was pointed out by Bruch and Tjon [8] who considered qualitatively the binding properties of three identical bosons interacting via two-body potential in 2D. They found no Efimov states in 2D. Cabral and Bruch [9] also studied helium trimers in 2D and confirmed a larger binding energy for helium-4

trimer than in 3D. They also concluded that fermion helium trimers probably did not exist in 2D.

Recently Krischnamachari and Chester [39] have studied liquid puddles of ^4He and boson ^3He . They have estimated that ^3He does not bind in 2D. Contrary to this conclusion a variational calculation showing the binding of both ^3He dimer and trimer in 2D has been performed [40].

Dimers, trimers, and tetramers may be thought as models for the interactions between many helium atoms in specific real physical environment. Here, for example, one has in mind solid matrices, where these systems form the condensation seed for helium clusters, then nanotubes, with a diameter between 3 Å and 100 Å and generally “condensation” on a solid or liquid substrate.

In a dilute solution of ^3He in liquid ^4He each ^3He prefers to float on the surface of the ^4He rather than to be dissolved in the bulk [41]. Thus one may imagine atoms at low temperatures (below 0.1 K), on the surface of bulk liquid ^4He , as a fermion system of spin-1/2 (or spin-3/2) particles moving in two-dimensional space. ^3He and ^4He adsorbed on the graphite surface form other almost 2D systems that are being extensively studied [42–44].

In this paper we study helium trimers and tetramers in infinite 2D space and in three holding potentials: (1). circle with hard core on its edge, which is pure 2D confined space, (2). Gaussian potential [45], and (3). “helium-on-graphite” potential [43]; last two potentials keep the particles close to a surface and define quasi-2D space. Dimer binding energies of ^3He and ^4He on graphite are also obtained. Binding energies of mixed molecules of three and four helium atoms in infinite 2D space are calculated as well. In Sec. II we define Hamiltonians, wave functions, and general expression that is used in the calculation of the energy. A short description of employed Monte Carlo numerical procedures and results are presented in Sec. III. We summarize and discuss the results in Sec. IV.

*Electronic address: leandra@pmfst.hr

†Electronic address: kilic@pmfst.hr

II. BASIC RELATIONS

We consider helium atoms as point particles. Atoms of ^4He are bosons with spin zero and atoms of ^3He are fermions with spin 1/2, interacting via spin-independent central pair potential. In general form Hamiltonian of our systems reads

$$H = -\frac{\hbar^2}{2m} \sum_{i=1}^n \Delta_i + \sum_{i<j=1}^n V(r_{ij}) + \sum_{i=1}^n V_{ext}(r_i). \quad (1)$$

Taking the corresponding mass for $n=3$ (4) Hamiltonian is adapted to trimer (tetramer) of helium 3 and helium 4. Potential $V(r_{ij})$ describes the interaction between two particles and in this paper we take Korona *et al.* symmetry-adapted perturbation theory (SAPT) potential [46]. $V_{ext}(r_i)$ is external holding potential.

We consider three types of external potentials independently. The first holding potential is a pure two dimensional that keeps particles to move in a circle of the radius R ; it is defined by

$$V_{ext}(r_i) = \begin{cases} \infty & \text{for } r_i \geq R \\ 0 & \text{for } r_i < R, \end{cases} \quad (2)$$

where r_i is two-dimensional position of atom i . In this potential the solution of the Schrödinger equation for the ground state of a particle is $J_0(Kr)$ with the energy $\hbar^2 K^2/2m$. J_0 is Bessel function and $K=2.404826/R$. The second is harmonic holding potential in 3D

$$V(z_i) = \frac{1}{2} m \omega_0^2 z_i^2, \quad (3)$$

for which the solution of Schrödinger equation,

$$-\frac{\hbar^2}{2m} \Delta \phi_0(z) + V(z) \phi_0(z) = \epsilon \phi_0(z), \quad (4)$$

is

$$\phi_0(z) = \frac{1}{a^{1/2} \pi^{1/4}} \exp(-z^2/2a^2), \quad (5)$$

where effective width is $a = (\hbar/m\omega_0)^{1/2}$, and z_i is the ordinate of three-dimensional position of atom i . For the smaller effective widths (say up to 3 Å) three-dimensional space is reduced to quasi-two-dimensional. The third holding potential is a realistic one, by Joly and co-worker. [43], that describes one helium atom on graphite substrate

$$V_{ext}(z_i) = A \exp(-\alpha z_i) - \frac{C_3}{z_i^3} - \frac{C_4}{z_i^4}, \quad (6)$$

where $A = 2.263439987 \times 10^6$ K, $\alpha = 3.715 \text{ \AA}^{-1}$, $C_3 = 1.827532376 \times 10^3 \text{ \AA}^3$ K, $C_4 = 1.029154519 \times 10^4 \text{ \AA}^3$ K, z_i is the ordinate of atom i , perpendicular to the graphite surface.

In a numerical solution of Schrödinger equation for the ground state of a ^3He atom in the potential (6) we obtained:

the value of the energy -135.8707 K and the corresponding function (data set). Using Gnufit we managed to fit the analytical function

$$\phi(z) = \exp[a_1 e^{-a_2 z} - a_3 z], \quad (7)$$

to the data set representing the wave function. This analytical form of the wave function with the obtained parameters $a_1 = 210.808$, $a_2 = 1.63445 \text{ \AA}^{-1}$, $a_3 = 3.50135 \text{ \AA}^{-1}$, can be considered as an excellent approximate function. Namely, it reproduces almost the same shape as the numerical solution and it gives the energy -135.86835 K. So Eq. (7) may be considered as ground-state eigenfunction.

In both stages of the calculation we sum the local energies $E_L = (H\Psi)/\Psi$,

$$E[\Psi] = \lim_{M \rightarrow \infty} \frac{1}{M} \sum_{i=1}^M E_L(X_i), \quad (8)$$

where Ψ is the trial wave function and sample points are taken from the distribution Ψ^2 in simple variational Monte Carlo (VMC) and from the mixed distribution $\Psi\Psi_g$ in diffusion Monte Carlo (DMC); Ψ_g is the exact ground-state wave function.

In the definition of binding energy among atoms in confined space we subtract the energy of every single particle in holding potential [47].

Let us now define wave functions.

1. Boson wave functions

A very good trial wave function describing ground state of helium-4 dimer and molecule of one atom of helium 4 and one atom of helium 3, was obtained and used in Ref. [47]. Short-range correlations between two atoms are described as in Jastrow-Feenberg (JF) wave function for liquid helium state. Long-range correlations are introduced by decreasing exponential function. Thus the product of short- and long-range correlations is defined by the function

$$f(r_{ij}) = \exp\left[-\left(\frac{\alpha}{r_{ij}}\right)^\gamma - s r_{ij}\right], \quad (9)$$

where r_{ij} is the interparticle spacing, α , γ , and s are variational parameters.

A comparison with numerical solution of Schrödinger equation showed that the best trial form for a dimer in 2D is the function $f(r)$, divided by the square root of the interparticle distance. In the case of the dimer in 3D we found that a good trial wave function is obtained if $f(r)$ is divided by the interparticle distance. Bruch [25] also used such function in the study of helium-4 trimer in 3D. Therefore, we define symmetric wave functions for helium-4 trimer ($n=3$) and tetramer ($n=4$) in the form

$$\Psi_0 = \prod_{i<j}^n F(r_{ij}), \quad (10)$$

where

$$F(r_{ij}) = \begin{cases} \frac{f(r_{ij})}{r_{ij}} & \text{in 3D} \\ \frac{f(r_{ij})}{\sqrt{r_{ij}}} & \text{in 2D.} \end{cases} \quad (11)$$

In holding potentials the corresponding wave functions have the form in a circle,

$$\Psi_0 = \prod_{i<j}^n F(r_{ij}) \prod_{i=1}^n J_0(Kr_i), \quad (12)$$

in harmonic potential,

$$\Psi_0 = \prod_{i<j}^n F(r_{ij}) \prod_{i=1}^n \phi_0(z_i), \quad (13)$$

and on graphite,

$$\Psi_0 = \prod_{i<j}^n F(r_{ij}) \prod_{i=1}^n \phi(z_i), \quad (14)$$

where again $n=3$ is for the trimer and $n=4$ for the tetramer.

2. Fermion wave functions

Since ^3He atoms are fermions, trimers and tetramers should be described by antisymmetric wave functions. The main problem here is to obtain a good correlation function. It is a known fact that there is no binding state of fermion helium dimer and trimer in infinite 3D space [5]. Our experience in 2D showed that radial function (9), although very good for helium-4 dimer and $^4\text{He}\text{-}^3\text{He}$ molecule, was not good enough to give bound state of the fermion helium dimer. This dimer is very large (the largest diatomic molecule in the ground state we know) and behavior of the correlation function in between short and long range is crucial. Using Gnuplot graphics and data from numerical solution of Schrödinger equation for fermion helium dimer [47], we were able to construct the following trial two-body wave function [40,48]:

$$f_f(r) = \sum_{i=1}^6 f_i(r). \quad (15)$$

The explicit form of summands is given in the Appendix. The function and its first derivative are plotted in Fig. 1. Variational fermion wave functions are taken over from Bruch and co-workers for trimer [5,9] and from [11,49] for tetramer. Let us call them Jastrow-Feenberg-Bruch (JFB) wave functions. In all expressions the correlation form (15) must be included. They are as follows:

(a) Trimer (spin 1/2)

$$\Psi = \phi_a X_s + \phi_s X_a, \quad (16)$$

where X_s and X_a are spin doublets, symmetric and antisymmetric, respectively, under exchange of particles 1 and 2 while ϕ_a and ϕ_s are space wave functions that are, respec-

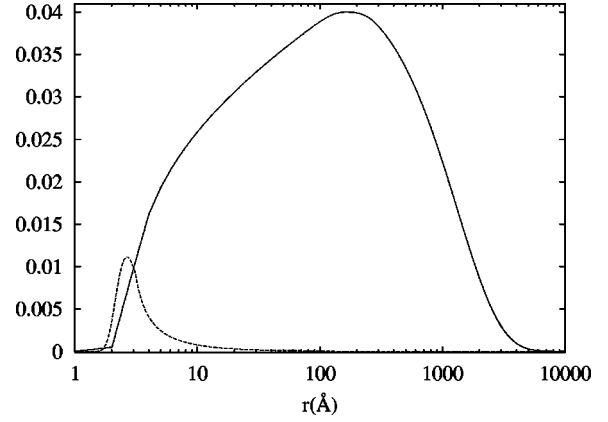


FIG. 1. The fermion radial wave function $f_f(r)$ (solid line) and first derivative $f'_f(r)$ (dashed line) for the parameters derived in energy-minimization procedure of the $^3\text{He}_3$ spin 1/2.

tively, antisymmetric and symmetric under exchange of particles 1 and 2. Spin-(+1/2) projections of the doublets are

$$X_a(s_z=1/2) = \frac{1}{\sqrt{2}}(\alpha_1\beta_2\alpha_3 - \beta_1\alpha_2\alpha_3), \quad (17)$$

$$X_s(s_z=1/2) = \frac{1}{\sqrt{6}}(2\alpha_1\alpha_2\beta_3 - \alpha_1\beta_2\alpha_3 - \beta_1\alpha_2\alpha_3), \quad (18)$$

where $\alpha_i(\beta_i)$ are the usual spin-up (down) eigenstates of a spin-1/2 particle and the subscript i is particle label. In the calculation for the space wave functions we combine the following forms:

$$\phi_a = \phi_a^y \Psi_0 = (y_1 - y_2) \Psi_0$$

or

$$\phi_a = \phi_a^x \Psi_0 = (x_1 - x_2) \Psi_0, \quad (19)$$

and

$$\phi_s = \phi_s^y \Psi_0 = \frac{1}{\sqrt{3}}[(y_3 - y_1) + (y_3 - y_2)] \Psi_0$$

or

$$\phi_s = \phi_s^x \Psi_0 = \frac{1}{\sqrt{3}}[(x_3 - x_1) + (x_3 - x_2)] \Psi_0. \quad (20)$$

Function Ψ_0 is given in the relation (10), where the function (15) is introduced instead of the function (9).

(b) trimer (spin 3/2)

$$\Psi = \phi_a X_s, \quad (21)$$

where

$$\phi_a = (x_1 y_3 - x_3 y_1 + x_2 y_1 - x_1 y_2 + x_3 y_2 - x_2 y_3) \Psi_0, \quad (22)$$

$$X_s(s_z=3/2) = \alpha_1 \alpha_2 \alpha_3, \quad (23)$$

(c) tetramer (spin 0)

$$\Psi = R_a X_{s4} + R_s X_{a4}, \quad (24)$$

where

$$X_{a4} = \frac{1}{2} (\alpha_1 \beta_2 \alpha_3 \beta_4 + \beta_1 \alpha_2 \beta_3 \alpha_4 - \alpha_1 \beta_2 \beta_3 \alpha_4 - \beta_1 \alpha_2 \alpha_3 \beta_4), \quad (25)$$

$$X_{s4} = \frac{1}{\sqrt{12}} (\alpha_1 \beta_2 \alpha_3 \beta_4 + \beta_1 \alpha_2 \beta_3 \alpha_4 + \alpha_1 \beta_2 \beta_3 \alpha_4 + \beta_1 \alpha_2 \alpha_3 \beta_4 - 2 \alpha_1 \alpha_2 \beta_3 \beta_4 - 2 \beta_1 \beta_2 \alpha_3 \alpha_4), \quad (26)$$

$$R_s = \frac{1}{\sqrt{3}} \left(\vec{r}_{32} \vec{r}_{14} - \frac{1}{2} \vec{r}_{12} \vec{r}_{34} \right) \Psi_0, \quad (27)$$

$$R_a = \frac{1}{2} (\vec{r}_{12} \vec{r}_{34}) \Psi_0. \quad (28)$$

The function Ψ_0 is symmetric and its form depends on the confinement type.

3. “Dimerlike” fermion wave functions

Binding of ^3He trimer and tetramer may be qualitatively studied in the relation with the dimer binding. Namely, wave functions (16), (21), and (24) treat all atoms in a molecule as in JF many-body problem, i.e., the correlations among all particles are described quite symmetrically. Contrary to the Jastrow-Feenberg-Bruch-type functions we construct functions that express dimer correlations in each summand explicitly. They may be called “dimerlike” wave functions.

For trimer spin 1/2 it is

$$\Psi(123) = \psi(12)\varphi(3)\chi(12)\alpha(3) - \psi(13)\varphi(2)\chi(13)\alpha(2) + \psi(23)\varphi(1)\chi(23)\alpha(1), \quad (29)$$

where

$$\chi(ij) = \frac{1}{\sqrt{2}} (\alpha_i \beta_j - \beta_i \alpha_j), \quad (30)$$

two-body correlation function $\psi(r_{ij})$ is given by relations (11) and (15), and $\varphi(i)$ is the wave function of free particle i .

Similarly, for the tetramer we take

$$\begin{aligned} \Psi(1234) = & \psi(12)\psi(34)\chi(12)\chi(34) \\ & - \psi(13)\psi(24)\chi(13)\chi(24) \\ & + \psi(14)\psi(23)\chi(14)\chi(23). \end{aligned} \quad (31)$$

4. Mixed-molecule wave functions

Wave functions for study of mixed molecules in infinite 2D space, each containing three and four nonidentical helium atoms, have been formed from the above two-body correlation functions. They are

TABLE I. The ^3He and ^4He trimer and tetramer binding energies (in mK) in infinite 2D space.

	^4He	^3He	
Trimer	-183(1)	-0.013(1) ^a	-0.020(1) ^b
Tetramer	-435(1)	-0.021(2) ^a	-0.040(1) ^b

^aJFB function.

^b“Dimerlike” function.

$$\Psi(1;23) = F_m(r_{12})F_m(r_{13})F(r_{23}), \quad (32)$$

$$\Psi(12;3) = F_f(r_{12})F_m(r_{13})F_m(r_{23}), \quad (33)$$

for ^3He - $^4\text{He}_2$ and $^3\text{He}_2$ - ^4He , respectively, and

$$\Psi(1;234) = \left(\prod_{j=2}^4 F_m(r_{1j}) \right) F(r_{23})F(r_{24})F(r_{34}), \quad (34)$$

$$\Psi(12;34) = F_f(r_{12})F_m(r_{13})F_m(r_{14})F_m(r_{23})F_m(r_{24})F(r_{34}), \quad (35)$$

$$\Psi(123;4) = \Psi_3(123) \prod_{j=1}^3 F_m(r_{j4}), \quad (36)$$

for ^3He - $^4\text{He}_3$, $^3\text{He}_2$ - $^4\text{He}_2$, and $^3\text{He}_3$ - ^4He , respectively. $F(r)$ is given in the relation (11). $F_m(r)$ has the same form as $F(r)$, with new variational parameters α_m, γ_m, s_m . $F_f(r)$ is also given in the relation (11) where function (15) is introduced instead of Eq. (9). $\Psi_3(123)$ is ^3He trimer wave function given in the relation (16).

III. NUMERICAL PROCEDURE AND RESULTS

Monte Carlo procedure is one of the most employed numerical methods for solving few-body problems nowadays. To obtain effectiveness and precision we perform all calculations in two stages. In the first stage VMC with simple sampling is used in order to obtain: (a) minimizing parameters in variational wave function, (b) initial trial energy, and (c) initial walkers configuration. All these are used in the second stage that is DMC. The number of walkers and steps in any Markov chain depends on the space where atoms move and on the type of the atoms. We find that acceptance about 50% in VMC and above 99.5% in DMC gives a good stabilization of the results. For helium-4 atoms we take from 500 up to 1000 walkers and for helium-3 atoms we find that 3000–5000 walkers is enough. In particular, due to very small binding energies for ^3He trimer and tetramer in 2D we performed the calculation with six different blocks of 5000 walkers using different random-number seeds. Generally speaking the calculation for helium 3 due to extended wave

TABLE II. Binding energies (in mK) of mixed helium molecules in infinite 2D space.

^3He - $^4\text{He}_2$	$^3\text{He}_2$ - ^4He	^3He - $^4\text{He}_3$	$^3\text{He}_2$ - $^4\text{He}_2$	$^3\text{He}_3$ - ^4He
-74.3(4)	-14(1)	-254(4)	-118(2)	-11(1)

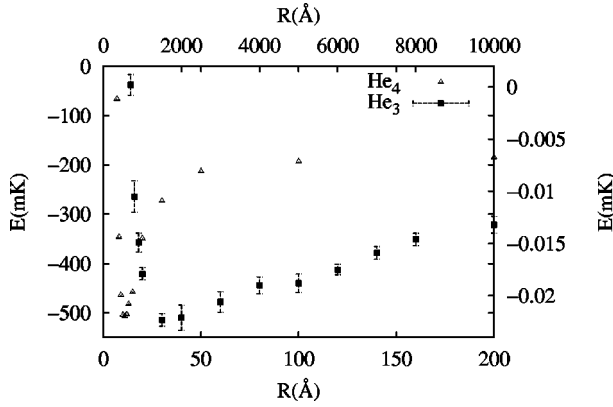


FIG. 2. The ${}^3\text{He}_3$ (upper and right scale) and ${}^4\text{He}_3$ (bottom and left scale) energy vs the radius of the circle. The errorbars for ${}^4\text{He}$ are smaller than the symbol size.

function asks for more walkers and more steps. The thermalization in every step is 10. Averaging data for the energy after an appropriate number of steps we are able to look at stabilization of the results. The number of total steps in DMC is between 5×10^5 and 2×10^6 . In most cases we had to calculate the energies for different time intervals that were used. In these cases the result is derived by the extrapolation to zero time step. Monte Carlo calculation is always time consuming. In our case for bosons we had to minimize over three parameters and for fermions over eleven parameters.

The results for the binding energy of ${}^3\text{He}$ and ${}^4\text{He}$ trimer and tetramer in 2D infinite space are presented in Table I and for mixed molecules in Table II. Let us mention that all calculations in holding potentials are performed using JFB functions.

Binding energies of both systems in the circle are shown in Fig. 2. In quasi-two-dimensional space energies are obtained for the width of 3 Å of harmonic holding potential (Table III).

The calculation of dimer and trimer binding energies of ${}^3\text{He}$ and ${}^4\text{He}$ on graphite are given in Table IV. We have also studied the effects of mass and spin on the binding of trimers.

In addition to the ground-state energies we have obtained the space distributions of atoms in our systems. The distributions of particle distances from the center of mass are shown in Figs. 3–5. The pair distribution functions are presented in Figs. 6 and 7.

An image of the arrangement of the atoms in a trimer may be obtained by the analysis of the atomic coordinates. A very

TABLE III. The ${}^3\text{He}$ and ${}^4\text{He}$ dimer, trimer, and tetramer binding energies (in mK) in harmonic holding potential with effective width of $a=3$ Å.

	${}^4\text{He}$	${}^3\text{He}$
Dimer	-101.84^a	-8.25^a
Trimer	$-482(2)$	$-8.6(7)$
Tetramer	$-1200(20)$	$-16.5(8)$

^aReference [45].

TABLE IV. The ${}^3\text{He}$ and ${}^4\text{He}$ dimer and trimer binding energies (in mK) on graphite.

	${}^4\text{He}$	${}^3\text{He}$
Dimer	$-43(2)$	$-0.045(8)$
Trimer	$-188(3)$	$-0.022(7)$

simple and still clear way is the introduction of a dynamic coordinates frame. In this frame one atom is situated in the origin, the second jumps along positive x axis and the third moves in the whole plane. Counting the coordinate projections of the third atom on the x axis, labeled x_p , and y axis, labeled y_p , during walk, is the basis for the calculation of the atomic distribution. Let us call it the “conditional” density. Figure 8 shows such a distribution for the trimer of ${}^4\text{He}$ in infinite 2D space. The same distribution is shown for ${}^3\text{He}$ trimer in Fig. 9; here due to extended helium-3 wavefunction the coordinates $x'_p = \pm[\log_{10}(|x_p| + 0.5) + 1/15]$ and $y'_p = \log_{10}(|y_p| + 0.5) + 1/15$ have been used. For simplicity x_p and y_p are here dimensionless, while x'_p and y'_p are in Å. Notice that x_p and x'_p have the same sign. It is also assumed $x'_p = 0$ for $|x_p| < 0.5$ and $y'_p = 0$ for $|y_p| < 0.5$. In order to learn more about the shape of trimers and tetramers we have also calculated the probability of specific configurations of atoms. In relation to this Fig. 4 represents the details of the Fig. 3 for ${}^4\text{He}$ tetramer.

All distributions are obtained by binning. In the case of pair and density distribution functions the bin size for ${}^4\text{He}$ is 0.01 Å and for ${}^3\text{He}$ 1 Å. For the conditional density we use the fixed bin size of 1 Å² for ${}^4\text{He}$ while the bin size for ${}^3\text{He}$ is variable and depends on the x'_p and y'_p .

Let us mention that distributions are normalized to one as follows:

$$\int_0^\infty P(r)rdr = 1, \quad \int_{-\infty}^\infty \int_0^\infty P(x_p, y_p) dx_p dy_p = 1,$$

$$\text{and} \quad \int_0^\infty \rho(r)rdr = 1.$$

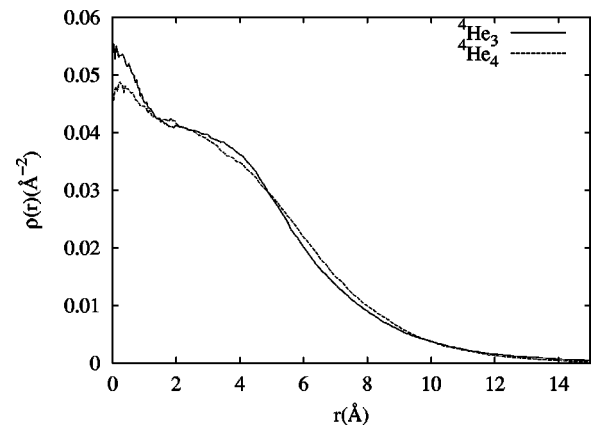


FIG. 3. The density of particles with respect to the center of mass for ${}^4\text{He}_3$ and ${}^4\text{He}_4$.

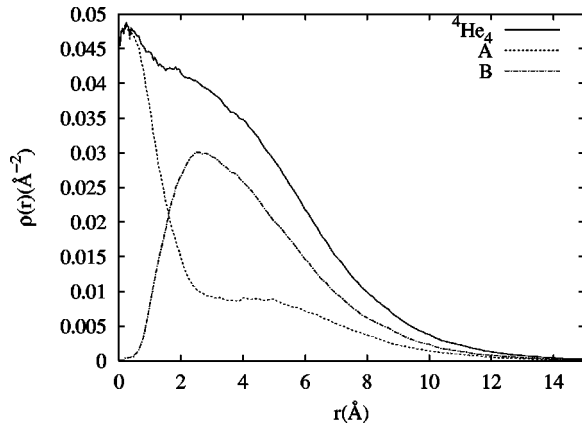


FIG. 4. The total density and the density of “A” and “B” configurations with respect to the center of mass for ${}^4\text{He}_4$.

Using mixed estimator one finds correct values for the energy, but obtains only an approximation (better than the VMC) for operators that do not commute with the Hamiltonian. This approximation is of the first order in the error of the trial wave function. To obtain a better estimate for various radial distribution functions it is common to use the so-called “second-order approximation” [50],

$$\langle A \rangle = 2\langle A \rangle_{DMC} - \langle A \rangle_{VMC}, \quad (37)$$

where A is a local operator. The value $\langle A \rangle$ differs from the exact expectation value of A in the integral of second order in the $\Psi_g - \Psi$. In our calculations for ${}^4\text{He}$, VMC, DMC, and second-order distribution functions are very close, which is due to good trial wave functions. For ${}^3\text{He}$ however, the differences between DMC and VMC at some distances are significant, but the average distance among particles from VMC to DMC is not changed so much.

For the sake of clarity errorbars on the Figs. 3–10 are not shown. In the case of ${}^4\text{He}$ molecules they vary from 2–5% depending on the corresponding distance. For ${}^3\text{He}$ systems errors are on the average 10%.

The calculations were performed using origin 3700 super-computer at Johannes Kepler University in Linz, Austria.

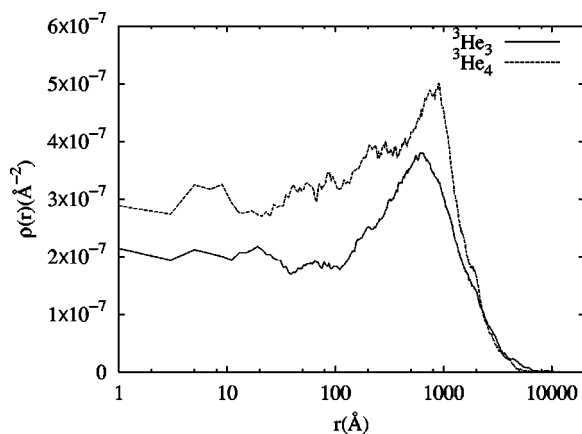


FIG. 5. The density of particles with respect to the center of mass for ${}^3\text{He}_3$ and ${}^3\text{He}_4$.

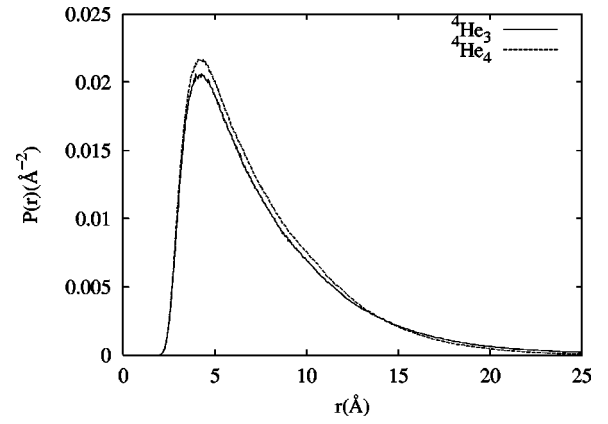


FIG. 6. The pair distribution function for ${}^4\text{He}_3$ and ${}^4\text{He}_4$.

IV. DISCUSSION

It is shown that atoms of ${}^4\text{He}$ form stable trimers and tetramers in infinite 2D space. Binding energies are $-183(1)$ mK (trimer) and $-435(1)$ mK (tetramer).

In the case of ${}^3\text{He}_N$ atoms in infinite 2D space both types of wave functions, JFB and dimerlike, give bound states. For JFB wave functions binding energies are $-0.013(1)$ mK for $N=3$ and spin 1/2 and $-0.021(2)$ mK for $N=4$ and spin 0. At the same time dimerlike wave functions give lower energies: $-0.020(1)$ mK for $N=3$ and spin 1/2 and $-0.040(1)$ mK for $N=4$ and spin 0.

For comparison we cite here the dimer binding energies [47]: -40.7 mK (${}^4\text{He}$) and -0.02 mK (${}^3\text{He}$); let us mention that using our procedure we reproduce the same results.

In order to compare our results with others we have first used JFB wave functions.

In the consideration of the binding-energy dependence on the mass and the statistics in trimers the following energies are obtained: $-0.25(1)$ mK for boson ${}^3\text{He}$ and $-29(1)$ mK for fermion ${}^4\text{He}$. A comparison with the results in the Table I shows that mass effect in boson trimer lowers binding 732 times and in fermion trimer increases binding around 2200 times. Similarly we find that statistics effect in ${}^3\text{He}_3$ decreases binding 19 times and in ${}^4\text{He}_3$ 6.3 times. Recently, Krishnamachari and Chester [39] have obtained

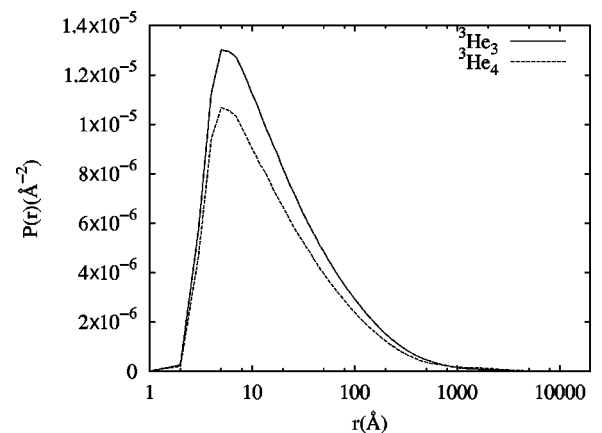


FIG. 7. The pair distribution function for ${}^3\text{He}_3$ and ${}^3\text{He}_4$.

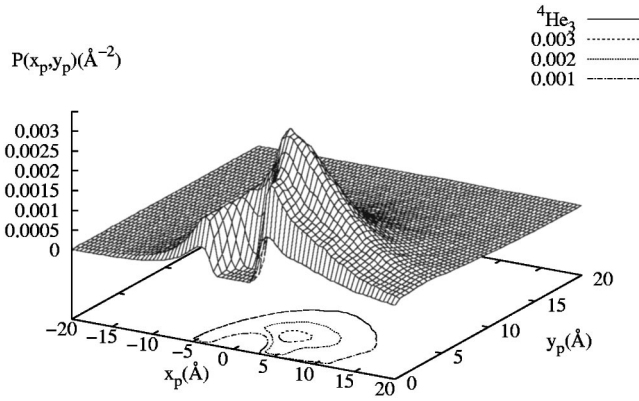


FIG. 8. The conditional density function presenting the distribution of one particle in ${}^4\text{He}_3$ when one of the other two particles is situated in the origin and the second moves along the positive side of x axis. x_p and y_p are projections of considered particle on the axes x and y , respectively.

that the minimum number of mass-3 bosons that bind in 2D is greater than 11. On the other hand, we have found the bound states for both ${}^3\text{He}$ dimer and trimer (as a boson and a fermion). It is possible that their wave function was not extended enough for liquid puddles having very small number of particles.

Calculating density functions and some other related local quantities we are able to get an insight into the structure of trimers and tetramers.

Consider first ${}^4\text{He}$ trimer. The average distance between atoms in ${}^4\text{He}$ trimer is 9.5 Å that is about 1.4 times less than in ${}^4\text{He}$ dimer. Root-mean-square (rms) deviation is 3.9 Å. A peak for small r in Fig. 3 corresponds to the contributions from linear configurations. However, trimer does not spend much time in such configurations. Namely, the number of trimer walkers that have two angles less than 1° is 1%, and with two angles less than 5° is 5%. We may conclude that about 95% of its time the trimer is a nonlinear molecule.

In ${}^4\text{He}$ tetramer the average distance between atoms is 9.1 Å and rms deviation 2.4 Å. In this case one may study two types of the configurations, say “A” and “B.” Let A

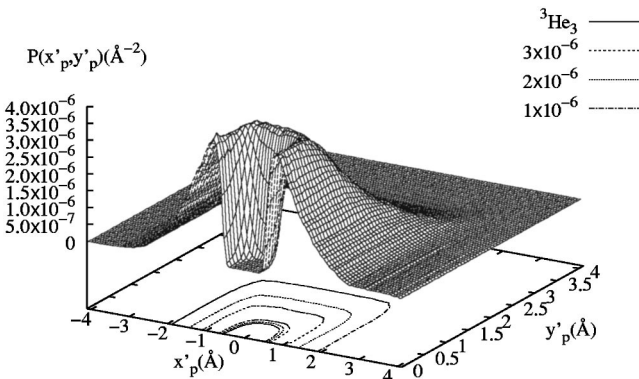


FIG. 9. The conditional density function for ${}^3\text{He}_3$. Due to extended helium-3 wave function the coordinates are defined as follows: $x'_p = \pm[\log_{10}(|x_p| + 0.5) + 1/15]$ and $y'_p = \log_{10}(y_p + 0.5) + 1/15$.

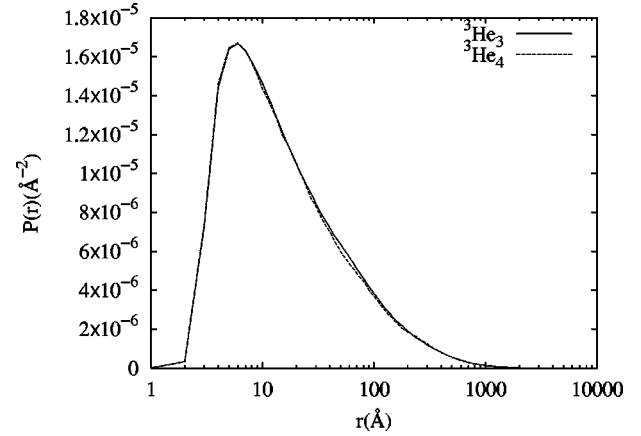


FIG. 10. The pair distribution function of ${}^3\text{He}_3$ and ${}^3\text{He}_4$ for “dimerlike” function. For both systems $\int_0^{10^4} P(r)rdr = 1/3$ that indicates the formation of dimers.

represent all the configurations in which one particle is within a triangle formed by the other three. The B comprises all other cases, thus pure quadrilaterals. We find that 35% of the walkers are in the configuration A and 65% are in the B . This is shown in Fig. 4.

The average distance between atoms of 4300 Å in ${}^3\text{He}_3$ is about 8.3 times greater than in ${}^3\text{He}$ dimer. The value of rms deviation is 1600 Å. The number of nonlinear walkers is almost the same as in the case of ${}^4\text{He}$ trimer, (94%). However, its shape is different from the ${}^4\text{He}$ trimer. Namely, the number of the configurations with all angles in the triangle greater than 15° is 16% for ${}^3\text{He}_3$ and 69% for ${}^4\text{He}_3$, signifying that the form of ${}^3\text{He}_3$ is far from resembling the equilateral triangle. Moreover, the number of the configurations with the distance between two particles less than 1000 Å and the other two interparticle distances bigger than 3000 Å is 46%. This also may be seen from the shape of the pair distribution function, Fig. 7, which for interparticle distances less than 1000 Å closely resembles the dimer pair distribution function.

${}^3\text{He}_4$ has the average distance between atoms 3100 Å and rms deviation is 1500 Å. In this case the configuration A comprises 22%, while in B there are 78%. Let us define the bond angle as the angle between \mathbf{r}_{ij} and \mathbf{r}_{ik} . If we now consider the configurations with at least one of the bond angles smaller than 1° , we find 7% of them for ${}^4\text{He}$ and 28% for ${}^3\text{He}$ tetramer. Such configurations occur when there are at least two particles close and one (of the remaining two) relatively far away.

In conclusion we may say that ${}^4\text{He}$ trimers and tetramers in 2D space are floppy molecules. Trimers on the average form triangles and tetramers quadrilaterals. However, ${}^4\text{He}$ trimers and tetramers are much more compact and symmetric than ${}^3\text{He}_3$ and ${}^3\text{He}_4$. Namely, ${}^3\text{He}_3$ shows a slight indication to have two particles closer (like one dimer) and the third particle relatively far away. Similarly, two separate pairs of particles occasionally form ${}^3\text{He}_4$. Having in mind the above observation and the values of ${}^3\text{He}$ dimer, ${}^3\text{He}_3$ and ${}^3\text{He}_4$ binding energies we have studied particle distributions using “dimerlike” functions. The results given in Fig. 10 show that

TABLE V. Binding energies (in mK) of helium molecules in infinite 3D space taken from the recent literature.

$^4\text{He}_3$	-126.4 [32]	-125 [26]	-125.9 [28]	-126.4 [27]
	-125.2 [22]	-219.1 [24]	-129 [20]	-131 [25]
$^3\text{He}-^4\text{He}_2$	-14.2 [32]	-13.66 [22]		
$^4\text{He}_4$	-559.1 [32]	-557 [26]	-559.2 [20]	
$^3\text{He}-^4\text{He}_3$	-296.7 [32]			
$^3\text{He}_2-^4\text{He}_2$	-102 [32]			

$^3\text{He}_3$ has the structure of one dimer and one separate particle while $^3\text{He}_4$ has the form of two separate dimers. The same conclusion follows from the comparison with the dimer binding energies. Finally, as binding energy for “dimerlike” wave functions is below the binding energy for JFB wave functions we conclude that the ground state of three and four ^3He atoms in infinite 2D is dimerized. It means three atoms form a dimer and a free particle, while four atoms form two dimers. It is interesting to notice that quite recent study [51] on 2D $^3\text{He}-^4\text{He}$ mixtures has shown the formation of ^3He dimers within the ^4He background for small ^3He concentrations.

To the best of our knowledge no results for the binding energy of three and four helium atoms of any sort in infinite 2D space have been obtained using modern potentials. In older papers [9,10] only the binding of helium-4 trimer and tetramer has been obtained. The agreement with our results is only qualitative.

It is interesting to compare the binding in infinite 2D and 3D space. Let us cite the recent results of other authors in 3D (Table V). Our results (Tables I and II) show that all three-atomic helium systems are bound stronger in 2D than in 3D. Notice that in contrast to 3D all three-atomic molecules are bound in 2D.

Concerning four-atomic molecules in 3D binding has been obtained only for $^4\text{He}_4$, $^3\text{He}-^4\text{He}_3$, and $^3\text{He}_2-^4\text{He}_2$. Again all four-atomic molecules are bound in 2D. But in this case molecules $^4\text{He}_4$ and $^3\text{He}-^4\text{He}_3$ are bound stronger in 3D.

In circular confined 2D space $^4\text{He}_3$ and $^3\text{He}_3$ show similar behavior as dimers [47]; binding is stronger for some values of the radius of the circle. In the limit $R \rightarrow \infty$, which is nearly achieved for $R=10\,000$ Å in case of $^3\text{He}_3$, and for $R=200$ Å in case of $^4\text{He}_3$, the trimer binding energies in infinite space are obtained. It is interesting to notice that $^3\text{He}_3$ is not bound for $R < 700$ Å and that the increase in the binding energy is much smaller than for the dimer [47].

In quasi-2D space derived by holding harmonic potential, with width of 3 Å, binding is drastically increased. Binding energies of ^4He trimer and tetramer are $-482(2)$ mK and $-1200(20)$ mK, respectively. In the same holding potential binding energies of $^3\text{He}_3$ and $^3\text{He}_4$ are $-8.6(7)$ mK and $-16.5(8)$ mK, respectively. $^3\text{He}_3$ and $^3\text{He}_2$ have the same binding energy (up to the error width), and $^3\text{He}_4$ has twice the dimer energy.

In helium-on-graphite potential binding of ^4He is almost the same as in 2D: for the dimer it is $-43(2)$ mK and for the trimer $-188(3)$ mK. In Ref. [44] a ^4He film on graphite

was studied. It was found that its properties are very close to 2D helium.

For ^3He we find that the dimer binding is increased two times when compared to pure infinite 2D and it is $-0.045(8)$ mK; for $^3\text{He}_3$ it is $-0.022(7)$ mK. But, the calculation of $^3\text{He}_3$ energy is very unstable so we can only say that it seems to be less bound than the dimer.

Different behavior of molecules in harmonic and helium-on-graphite potential may be explained. Binding of one helium atom on graphite substrate is relatively strong and localized. One can imagine that atoms move in a thin plane layer that is parallel to the substrate plane and about 3 Å away from it. The Gaussian wave function for $a=3$ Å has large extension in comparison with the case of helium-on-graphite potential and thus provides more space for the movement in the z direction. In harmonic potential maximal dimer binding [45] was obtained for the potential width of about $a=3.2$ Å. There it was shown that taking smaller widths binding becomes weaker and in the limit of $a \rightarrow 0$ gains the value as in the case of infinite 2D space.

Brami and co-workers have studied in a VMC calculation the binding of ^3He adsorbed on graphite. Taking into account the delocalization of atoms in the z direction they showed that ^3He atoms form a self-bound state. For the same system in infinite 2D space Miller and Nosanow [52] found no binding. We may notice that such behavior is not observed for a small number of particles, namely, we find binding in 2D in all studied cases. Furthermore, the enhancement of the binding on graphite is qualitatively confirmed.

It is known that Casimir retarded forces may affect the binding energy of these very large systems. We use two retarded potentials [53], SAPT1 and SAPT2. A reduction of the binding energy for helium-3 dimer in 2D of 6.6% for SAPT2 and 11.2% for SAPT1 is obtained. Our variational calculations shows that these percentages are slightly higher for $^3\text{He}_3$. We conclude that retarded forces do not change the general features of helium trimers and tetramers.

Cabral and Bruch [9] have showed that for some values of coupling constant the energy of $^3\text{He}_3$ with spin 3/2 is lower than for the $^3\text{He}_3$ with spin 1/2. We have not met this problem with real interaction. We have found that only $^3\text{He}_3$ with spin 1/2 is bound.

In connection with experimental observation of helium-3 molecules, it seems one should consider the adsorption on such substrates that provide wider wells than the graphite in the direction perpendicular to the substrate. Also, our results for helium 3 in circle suggest that if the surface of substrate has step irregularities on the scale less than about 1500 Å trimers are not self-bound. However, this number may be reduced when one considers the realistic substrates because the average distance among atoms in that case is considerably diminished.

Consideration of ^3He trimer and tetramer in holding potentials with dimerlike wave functions is in progress. Our preliminary results for binding energy in circle show stronger binding for the radius $R \approx 10\,000$ Å and weaker binding for $R < 5000$ Å when compared with results obtained by JFB wave functions.

ACKNOWLEDGMENTS

We are indebted to Professor E. Krotscheck for stimulating discussions and for the opportunity to use the supercomputer at Johannes Kepler University, Linz, Austria. We also would like to thank L. W. Bruch for valuable suggestions on the subject matter. A part of this work was done in Linz during a visit of one of us (L.V.) which was funded by Österreichische Austauschdienst. This research was supported by Ministry of Science and Technology of Republic of Croatia under Grant No. 177062.

APPENDIX

The explicit form of the summands in fermion correlation function (15) reads

$$f_1(r) = a_1 \exp\left[-\left(\frac{a_2}{r}\right)^{a_3}\right], \quad r \in [r_1, r_2],$$

$$f_2(r) = b_1 (\ln(r - b_2))^{b_3}, \quad r \in [r_2, r_3],$$

$$f_3(r) = c_1 \exp\left[-\left(\frac{|r_4 - r|}{c_2}\right)^{c_3}\right], \quad r \in [r_3, r_4 + \delta],$$

$$f_4(r) = d_1 \exp\left[-\left(\frac{r - r_4}{d_2}\right)^{d_3}\right], \quad r \in [r_4 + \delta, r_5],$$

$$f_5(r) = e_1 \exp\left[-\left(\frac{r - r_4}{e_2}\right)^{e_3}\right], \quad r \in [r_5, r_6],$$

$$f_6(r) = g_1 \sqrt{r} K_0(-sr), \quad r \in [r_6, \infty],$$

where K_0 is modified Bessel function. It has 24 parameters and 13 of them are independent.

-
- [1] S.Y. Larsen, Phys. Rev. **130**, 1424 (1963).
 [2] J.M. Blatt, J.N. Lyness, and S.Y. Larsen, Phys. Rev. **131**, 2131 (1963).
 [3] E.W. Schmid, J. Schwager, Y.C. Tang, and R.C. Herndon, Physica (Amsterdam) **31**, 1143 (1965).
 [4] L.W. Bruch and I.J. McGee, J. Chem. Phys. **59**, 409 (1973).
 [5] M.L. Cramer, L.W. Bruch, and F. Cabral, J. Chem. Phys. **67**, 1442 (1977).
 [6] T.K. Lim, S.K. Duffy, and W.C. Damert, Phys. Rev. Lett. **38**, 341 (1977).
 [7] S. Nakaishi, Y. Akaishi, H. Tanaka, and T.K. Lim, Phys. Lett. **68A**, 36 (1978).
 [8] L.W. Bruch and J.A. Tjon, Phys. Rev. A **19**, 425 (1979).
 [9] F. Cabral and L.W. Bruch, J. Chem. Phys. **70**, 4669 (1979).
 [10] T.K. Lim, S. Nakaishi, Y. Akaishi, and H. Tanaka, Phys. Rev. A **22**, 28 (1980).
 [11] S. Nakaishi-Maeda, T.K. Lim, and Y. Akaishi, J. Chem. Phys. **77**, 5581 (1982).
 [12] F. Luo, G. McBane, G. Kim, and C.F. Giese, J. Chem. Phys. **98**, 3564 (1993).
 [13] W. Schollkopf and J.P. Toennies, J. Chem. Phys. **104**, 1155 (1996).
 [14] F. Luo, C.F. Giese, and W.R. Gentry, J. Chem. Phys. **104**, 1151 (1996).
 [15] V.R. Pandharipande, S.C. Pieper, and R.B. Wiringa, Phys. Rev. B **34**, 4571 (1986).
 [16] M.V. Rama Krishna and K.B. Whaley, J. Chem. Phys. **93**, 6738 (1990).
 [17] S.A. Chin and E. Krotscheck, Phys. Rev. B **45**, 852 (1992).
 [18] R.N. Barnett and K.B. Whaley, Phys. Rev. A **47**, 4082 (1993).
 [19] M. Lewerenz, J. Chem. Phys. **106**, 4596 (1997).
 [20] R. Guardiola, M. Portesi, and J. Navarro, Phys. Rev. B **60**, 6288 (1999).
 [21] B.D. Esry, C.D. Lin, and C.H. Greene, Phys. Rev. A **54**, 394 (1996).
 [22] E. Nielsen, D.V. Fedorov, and A.S. Jensen, J. Phys. B **31**, 4085 (1998).
 [23] D. Bressanini, G. Fabbri, M. Mella, and G. Morosi, J. Chem. Phys. **111**, 6230 (1999).
 [24] T. Gonzalez-Lezana, J. Rubayo-Soneira, S. Miret-Artes, F.A. Gianturco, G. Delgado-Barrio, and P. Villarreal, Phys. Rev. Lett. **82**, 1648 (1999).
 [25] L. Bruch, J. Chem. Phys. **110**, 2410 (1999).
 [26] D. Blume and Chris H. Greene, J. Chem. Phys. **112**, 8053 (2000); D. Blume, Chris H. Greene, and B.D. Esry, *ibid.* **113**, 2145 (2000).
 [27] V. Roudnev and S. Yakovlev, Chem. Phys. Lett. **328**, 97 (2000).
 [28] A.K. Motovilov, W. Sandhas, S.A. Sofianos, and E.A. Kolganova, Eur. Phys. J. D **13**, 33 (2001).
 [29] V. Efimov, Phys. Lett. **33B**, 563 (1970); Yad. Fiz. **12**, 1080 (1970) [Sov. J. Nucl. Phys. **12**, 589 (1971)]; Nucl. Phys. A **210**, 157 (1973).
 [30] T. Gonzalez-Lezana, D. Lopez, S. Miret-Artes, F.A. Gianturco, G. Delgado-Barrio, and P. Villarreal, Chem. Phys. Lett. **335**, 105 (2000).
 [31] T.G. Lee, B.D. Esry, Bing-Cong Gou, and C.D. Lin, J. Phys. B **34**, L203 (2001).
 [32] D. Bressanini, M. Zavaglia, M. Mella, and G. Morosi, J. Chem. Phys. **112**, 717 (2000).
 [33] S. Stringari and J. Treiner, J. Chem. Phys. **87**, 5021 (1987).
 [34] S. Weisgerber and P.G. Reinhard, Z. Phys. D: At., Mol. Clusters **23**, 275 (1992).
 [35] M. Barranco, D.M. Jezek, E.S. Hernandez, J. Navarro, and Ll. Serra, Z. Phys. D: At., Mol. Clusters **28**, 257 (1993).
 [36] M. Barranco, J. Navarro, and A. Poves, Phys. Rev. Lett. **78**, 4729 (1997).
 [37] R. Guardiola and J. Navarro, Phys. Rev. Lett. **84**, 1144 (2000).
 [38] R. Guardiola, Phys. Rev. B **62**, 3416 (2000).
 [39] B. Krishnamachari and G.V. Chester, Phys. Rev. B **59**, 8852 (1999).
 [40] L. Vranješ and S. Kilić, J. Low Temp. Phys. **121**, 471 (2000).
 [41] A.F. Andreev, Zh. Éksp. Teor. Fiz. **50**, 1415 (1966) [Astrophys.

- J., Suppl. **23**, 939 (1966)]; R.B. Hallock, Phys. Today **51** (6), 30 (1988).
- [42] L.W. Bruch, M.W. Cole, and E. Zaremba, *Physical Adsorption: Forces and Phenomena* (Oxford, New York 1997).
- [43] F. Joly, C. Lhuillier, and B. Bami, Surf. Sci. **264**, 419 (1992); B. Bami, F. Joly, and C. Lhuillier, J. Low Temp. Phys. **94**, 63 (1994).
- [44] P.A. Whitlock, G.V. Chester, and B. Krishnamachari, Phys. Rev. B **58**, 8704 (1998).
- [45] S. Kilić, E. Krotscheck, and L. Vranješ, J. Low Temp. Phys. **119**, 715 (2000).
- [46] T. Korona, H.L. Williams, R. Bukowski, B. Jeziorski, and K. Szalewicz, J. Chem. Phys. **106**, 5109 (1997).
- [47] S. Kilić, E. Krotscheck, and R. Zillich, J. Low Temp. Phys. **116**, 245 (1999).
- [48] L. Vranješ and S. Kilić, Croat. Chem. Acta **73**, 1087 (2000).
- [49] L.W. Bruch, J. Chem. Phys. **72**, 5511 (1980).
- [50] K.S. Liu, M.H. Kalos, and G.V. Chester, Phys. Rev. A **10**, 303 (1974).
- [51] E. Krotscheck, J. Paaso, M. Saarela, and K. Schörkhuber, Phys. Rev. Lett. **85**, 2344 (2000); Phys. Rev. B **64**, 054504 (2001).
- [52] M.D. Miller and L.H. Nosanow, J. Low Temp. Phys. **32**, 145 (1978).
- [53] A.R. Janzen and R.A. Aziz, J. Chem. Phys. **107**, 914 (1997).